The Scd6 protein *x*RAPB has properties different from RAP55 in selecting mRNA for early translation or intracellular distribution in *Xenopus* oocytes

Michael Ladomery* and John Sommerville**

Biomedical Sciences Research Complex, Biomolecular Sciences Building, University of St Andrews, North Haugh, St Andrews, KY16 9TS, UK.

*Present address: Faculty of Health and Applied Sciences, University of the West of England, Coldharbour Lane, Bristol BS16 1QY, UK.
**Corresponding author (e-mail: js15@st-and.ac.uk)

Running title: Scd6 function in early oocytes

ABSTRACT

Oocytes accumulate mRNAs in the form of maternal ribonucleoprotein (RNP) particles, the protein components of which determine the location and stability of individual mRNAs prior to translation. Scd6 proteins, typified by RAP55, functions in a wide range of eukaryotes in repressing translation and relocating mRNPs to processing bodies and stress granules. Here we describe in *Xenopus laevis* a variant of RAP55, *x*RAPB, a member of the LSM14B family of proteins found in many other organisms, which also contains conserved Lsm and FDF domains but differs in containing fewer RGG repeats. *x*RAPB differs from *x*RAPA in other respects: it is expressed at high concentration earlier in oogenesis; it interacts specifically with the RNA helicase Xp54; it is a component of mRNP particles with a different size distribution; its over-expression leads to selective binding to translatable mRNA species without evidence of translation repression or mRNA degration. Since Xp54 is a dominant repressor of translation, activation appears to be effected by the dislocation of Xp54 from *x*RAPB.

1. Introduction

Throughout its existence, mRNA is associated with a wide range of proteins that determine its history and fate: co-transcriptional processing, nucleocytoplasmic transport, cellular localization and ability to be translated, result from a succession of interactions with protein factors and microRNAs (Muller-McNicoll and Neugebauer, 2013). Although many RNA sequence- and structure-specific proteins have been identified, little is known of the extent of heterogeneity in protein composition across the range of mRNP particles. In developing organisms, substantial amounts of mRNP are formed and stored until required for the synthesis of stage-specific proteins, whereas other mRNPs undergo immediate translation to establish the metabolic machinery (Lai and King, 2013). Not only the timing of translation initiation is determined but also the cessation of translation and mRNA decay. These and more subtle effects on the regulation of translation are incurred through the remodelling of mRNP particles. Key processes include: addition and removal of translation masking proteins, cytoplasmic regulation of poly(A) tail length, binding of translation initiation factors to the 5' cap structure, interaction of proteins bridging the 3' and 5' ends of the mRNA, mRNA localization, decapping and hydrolysis of the mRNA (Balagopal and Parker, 2009).

A paradigm for these various effects has been established from studies on oogenesis and early development of *Xenopus laevis*. Over a period of months, oocytes accumulate large numbers of non-translating, maternal mRNA molecules ($>10^{11}/$ oocyte) that are stored to be mobilized to polysomes during later stages of oogenesis, oocyte maturation and, after fertilization, early embryogenesis. During their storage phase, most of these mRNAs have relatively short poly(A) tails (10-30 residues) at their 3' termini (Cabada et al., 1977). Several abundant proteins are found to be associated with these maternal mRNAs to form large RNA-protein complexes which mostly sediment at 30-80 S and have a buoyant density in CsCl of 1.36 g.cm^{-3} (equivalent to a protein:RNA mass ratio of 4:1).

The four most abundant proteins have apparent (electrophoresis) molecular masses between 50-60 kDa (Darnbrough and Ford, 1981): the two slowest migrating were identified as cold-shock domain Y-box proteins, FRGY2a/b (YB2: Deschamps et al., 1992; Murray et al.,1992) and the next as the DEAD-box RNA helicase Xp54/Dhh1 (Ladomery et al., 1997). The fourth protein, of 52 kDa, described in this report as

*x*RAPB, is identified as a variant of RAP55 which is expressed in a wide range of organisms (Marnef et al., 2009). RAP55 was first identified as an RNA-associated protein expressed in oocytes of the amphibian *Pleurodeles waltl (*Lieb et al. 1998). Its orthologue is also expressed in *Xenopus* oocytes and is here referred to as *x*RAPA. All of the RAP55 proteins, including *x*RAPA and *x*RAPB, belong to the Scd6 family (Anantharaman and Aravind, 2004), characterized by a multidomain organization consisting of a conserved N-terminal Lsm domain and varied central and C-terminal regions defined by an FDF domain and RGG repeats (Albrecht and Lengauer, 2004). In this report we examine to what extent structural differences between *x*RAPA and *x*RAPB are reflected in differences in function.

RAP55/*x*RAPA has been shown to act as a translation repressor (Tanaka et al., 2006), as have the core mRNP proteins, YB2a/b (Kick et al.,1987: Matsumoto et al., 1996; Yurkova and Murray, 1997; Sommerville, 1999) and Xp54 (Minshall and Standart, 2004: Minshall et al., 2009), along with other mRNP proteins: CPEB (Minshall et al., 2007), 4-ET (Minshall et al., 2007) and P100/Pat1 (Marnef et al., 2010: Nakamura et al., 2010). However, other proteins, involved in mRNP trafficking and translation activation during oogenesis, have yet to be identified. Here we describe several features of *x*RAPB, which distinguish it from RAP55/*x*RAPA, specifically in having a key role in the regulation of mRNA metabolism during the early stages of oocyte development.

2. Materials and methods

2.1 Sequencing and cloning

Sequence information for *Xenopus laevis* *x*RAPA was obtained originally from EST clones BG408666 and BG486665 (European Bioinformatics Institute: www.ebi.ac.uk) which showed 74% protein identity with RAP55 of *Pleurodeles waltii* (UNIPROT Q9YH12; www.uniprot.org ; Lieb et al., 1998) and were known to be expressed in oocytes of *X. laevis*. A complete coding sequence was constructed from PCR reactions and later found to be identical at the protein level to that of IMAGE clone 3405473 (I.M.A.G.E Consortium: www.imageconsortium.org). *x*RAPB was initially detected by peptide sequencing of an mRNP protein of 52 kDa isolated from stage I oocytes of *X. laevis*: one of the peptide sequences, M/VEQAV, did not occur in either RAP55 or *x*RAPA, but was later detected in a human clone

(UNIPROT Q9BX40) which showed 45% identity with RAP55. *X. laevis* EST clones BI444610 and BG731378 were used to generate more extensive and overlapping sequences which were found to form a complete 5' insert in IMAGE clone 3473035 and a complete 3' insert in IMAGE clone 4674033, with a 299 bp overlap between them.

2.2 Expression vectors

PCR copies from cDNA clones encoding complete sequences of *x*RAPA and *x*RAPB were inserted into the pCS2*mt-SGP vector between the unique *Eco* RI site immediately downstream of the 6-times myc epitope and the Xba I site immediately upstream of the in-frame GFP sequence as described previously (Smillie and Sommerville, 2002). Stop codons were retained, or inserted, in a second set of vectors to generate transcripts lacking part or all of the GFP sequence. The pCGT vector expressing the complete sequences of Xp54 following a leader sequence encoding a T-epitope has been described (Smillie and Sommerville, 2002). All *in vivo* expression was driven from the CMV promoter. For *in vitro* expression, proteins were generated using the T_NT Quick Coupled Transcription/Translation System (Promega, Madison, WI) according to the supplier's instructions. Briefly, 0.5-2 μg of plasmid DNA was used in combination with 20 μCi of [^{35}S]-methionine (Redivue >1000 Ci/mmole; Amersham Biotech. GE Healthcare) and either T7 or SP6 RNA polymerase (Promega). After incubation at 30^oC for 90 min., the reactions were filtered through Sephadex G-50 (GE Healthcare) by centifugation in micro-pipette tips to separate the products from unincorporated radioactivity and small molecules. The integrity of radiolabelled products was checked by SDS-PAGE/autoradiography. Quantitation of incorporation was calculated by sampling aliquots in duplicate on to GF/A glass fibre filters (Whatman, GE Healthcare), with and without TCA precipitation and followed by scintillation counting according to supplier's instructions (Promega).

2.3 Morpholinos

Antisense morpholinos (Gene Tools, Philomath, OR) were directed against RNA sequences adjacent to translation start site (bold, where included):

Xp54 mRNA	3'**TAC**TCGTGGCGGTCTTGTCTCTTGG 5'
YB2 mRNA	3'CCTCG**TAC**TCACTCCGCCTTCGGGC 5'
*x*RAPB mRNA	3'GGTATCAGGTTTCTGCTCGTAG**TAC** 5'

*x*RAPA mRNA	3' GTAGGTAGGCCCTCTATCC**TAC**TCG 5'
pCS transcripts	3' GTTCGATGAACAAGAAAAACGACCT 5'
pCTG transcripts	3' **TAC**CGAAGATCCTACCGTAGCTACT 5'
Control	3' CCTCTTACCTCAGTTACAATTTATA 5'

All injected antisense morpholinos showed specific down-regulation of both endogenous and recombinant forms of the target proteins. No deleterious effect on oocytes were observed.

2.4 Oocyte isolation and extraction

Ovary was excised from immature *X. laevis* and oocytes were released and maintained in OR-2 medium and sorted into individual stages as described in detail (Sommerville, 2010). Pools of ~1000, 400, 100 and 40 oocytes, of stages I, II, III and IV were homogenized in HB: 0.1 M NaCl; 2 mM $MgCl_2$; 2 mM dithiothreitol, 20mM Tris-HCl, pH 7.5. Yolk and lipid were extracted with 1,1,2-trichlorotrifluoroethane (Evans and Kay, 1991). After centrifugation at 10,000 rpm for 15 min at $0^{o}C$ in a Sorvall SS-34 rotor, the clarified supernatant (SN10) was carefully removed. The extracts were maintained at $<2^{o}C$ throughout and adjusted to 40 units/□l RNasin (Promega) and where appropriate 5 mM EDTA (Sigma). Poly(A^{+}) RNP was bound to and eluted from oligo(dT) cellulose (Type 7; Pharmacia, GE Healthcare) as described previously (Ladomery et al., 1997). Typical recovery of poly(A^{+}) RNP from early stage oocytes was 250-350 μg/ml eluate.

2.4 Primary antibodies

Poly(A)$^{+}$RNP from early (stage I) oocytes was separated into a heat stable supernatant containing YB2a/b (Deschamps et al., 1992) and a heat-labile precipitate containing principally Xp54 and *x*RAPB. Antibodies were raised against the renatured proteins from these two fractions. Rabbits producing anti-YB2 generally gave equal reactivity to the a and b forms. Rabbits producing antibodies to the heat-labile proteins gave variable immuno-reactivities, either against Xp54 or *x*RAPB. Antibodies specific for Xp54 and p52 (*x*RAPB) were raised against gel-isolated proteins which were renatured by staged dilution from 8M urea into HB (Ladomery et al., 1997; Sommerville and Ladomery, 1996). Rabbit anti-ERK2 was obtained from

Santa Cruz Biotech. (Santa Cruz, CA) rabbit anti-phospho-MAP kinase from Cell Signalling (Danvers, MA). Rabbit anti-CPEB was kindly supplied by Laura Hake. Mouse monoclonal antibodies to the c-myc epitope (clone 9E10, Sigma-Aldrich, St Louis, MO) and the bacteriophage T7 epitope (Novagen, Merck, Darmstadt) were used as recommended.

2.6 Oocyte injection and radiolabelling

Stage IV oocytes from albino females were randomly distributed into four sets of 40-50 oocytes and each set was colour-coded using vital stains as described (Sommerville, 2010). The different sets were used for injection of different expression vectors or morpholinos or as controls. For over-expression studies, 10 nl aliquots containing ~10 pg of purified plasmid DNA were injected into the visible nucleus of colour-coded albino oocytes. Alternatively, RNA transcribed with T3 or T7 polymerase (MessageMachine, Ambion, Waltham, MA) from linearized vectors (10 □g in 20 nl) was injected into the cytoplasm. Antisense probes were synthesized by the same method but labeled with ^{32}[P]-CTP (0.1 mCi/ml at >1000 Ci/mmole; Amersham). For knock-down expression, antisense or control morpholinos (5 ng in 20 nl aliquots) were injected into the cytoplasm. After injection the oocytes were pooled and incubated together in OR-2 at room temperature (20-22 ^{o}C) for periods of 6 to 36 h. For metabolic labelling of proteins, sets of 25 colour-coded oocytes from each injection treatment were pooled and labelled by addition of 30 µl of [^{35}S]methionine (0.1 mCi/ml at >1000 Ci/mmole; Amersham) to a total volume of 3 ml of OR2 in 30 mm diameter plastic dishes. At each time point, 5 oocytes of each colour were removed with a minimum of liquid and rinsed twice in 2 ml of OR2 before transfer to a 0.5 ml centrifuge tube and frozen on dry ice. Quantitation of [^{35}S]methionine incorporation/protein synthesis was carried out as described (Keiper and Rhodes, 1997).

2.7 Immunoblotting

Proteins, equivalent to one oocyte, were separated by SDS-PAGE, transferred to nitrocellulose (0.45 micron, Pierce Biotech. Thermo Fisher) and immunoblotted as described previously (Ryan et al., 1999). Primary antisera or IgG were used at 1:5,000

or 1:10,000, secondary antibodies were goat-anti-rabbit or goat-anti-mouse IgG conjugated to IR Dye 800CW (Li-COR, Odyssey Biosciences, Lincoln, NE) and were all used at 1:40,000. Fluorescent bands were recorded using an Odyssey (Li-COR, Clx) infrared imaging system. All immunoblots shown are representative of those obtained from at least two experiments.

2.8 Immunostaining

Xenopus laevis ovary was fixed in 2% trichloroacetic acid, dehydrated, embedded in wax and sectioned on to glass slides. Dewaxed sections were rinsed with PBST, incubated for 1 hour at 20°C with anti-p54 diluted 1:200 in 10% FCS/PBST, rinsed five times in PBST for 10 min, then incubated with FITC-conjugated anti-rabbit IgG (Chemicon) diluted 1:200 in 10% FCS/PBST. After rinsing in PBST a further five times, the sections were mounted in 20% glycerol / PBST and viewed using an Olympus BX51 fluorescence microscope fitted with an SIS View Firewire CC-12 digital camera (Olympus Soft Imaging, 48149 Munster, Germany).

2.9 Immunoprecipitation

Antibodies were linked to ProSep-vA beads (Millipore, Watford, UK) and proteins or mRNP bound from HB containing 0.05% NP-40 (Sigma) and released as described previously (Ryan et al., 1999).

2.10 UV crosslinking

Samples of poly(A)$^{+}$RNP (25-35 μg in 100 μl HB) were placed in a silicone-treated glass depression tray seated on ice and irradiated with 254-nm light at 6,000 μW/cm^{2} for 5 min to establish protein-RNA crosslinks or 30 min to produce (more extensive) protein-protein crosslinks. Half of irradiated samples were treated with 1 mg/ml ribonuclease A at 37°C for 30 min to resolve close protein-protein association.

2.11 Rate sedimentation analysis

Clarified oocyte extracts and poly(A^{+}) fractions were layered on 10-25% glycerol gradients made up in: 0.1 M NaCl; 2 mM MgCl$_2$; 2 mM dithiothreitol; 20 mM Tris-HCl, pH 7.5 plus 0.05% NP-40, 40 units/$\square$l RNasin, with and without 50 μg/ml cycloheximide. For ribosome dissociation, MgCl$_2$ was replaced with 5 mM EDTA.

After centrifugation at 36,000 rpm in a 6 x 5 ml swing-out rotor (Beckman SW50Ti) at 0°C for 2-3 hours, the tube contents were fractionated. Fractions were analysed for proteins by immunoblotting. Sedimentation rates were calculated using 80S ribosomes and 60S and 40S ribosomal subunits run in parallel gradients and scanned through a flow cell measuring absorbance at 254 nm.

2.12 Density gradient centrifugation

Unfixed poly(A)$^+$RNP samples (50-100 μl) were layered on preformed gradients of 6-48% Cs_2SO_4 in 0.1% NP40 (Sigma) and 50 mM sodium phosphate, pH 7.0. After centrifugation at 35,000 rpm for 16 h at 18°C in a Beckman SW50Ti rotor, the tube contents were fractionated. Density values were obtained by refractometry. Each fraction was diluted with 3 vol. dH_2O, then RNP and proteins were ethanol precipitated, for protein extraction with addition of 10 μg of cytochrome C and for RNA extraction with 10 μg of yeast tRNA as carriers. Proteins were recovered from precipitatated fractions by standard preparation procedure for SDS-PAGE. RNA was recovered by SDS-protease treatment and standard phenol extraction. Unfixed poly(A)$^+$RNP was also separated on preformed CsCl gradients, formed and analysed as above.

2.13 RNA extraction, hybridization and RT-PCR

RNA was isolated extracts of 25 oocytes or acetone- or ethanol-precipitated gradient fractions or from immunoprecipitates raised in 250 μg HB plus 40 units/□l RNasin and from their supernatants, by addition of SDS to 1% followed by extractions with equal volumes of phenol-chloroform-isoamyl alcohol then chloform-isoamyl alcohol. 1/10th volume of 5M sodium acetate and 20 μg transfer RNA (Sigma) were added to the extracts and RNA was ethanol precipitated. Dried pellets were raised in RNase-free H_2O. RNA for hybridization analysis was either separated by gel electophoresis and transferred to nylon membranes or applied directly to the membranes using a Hybri-Slot Manifold (BRL, Bethesda) and hybridized with ^{32}[P]-CTP labelled antisense probes essentially as described (Sheets et al., 2010). RNA as a template for two-stage RT-PCR was used with random hexamers in the ImProm-II^{TM} Reverse Transcription System (Promega) to generate cDNA followed by amplification with GoTaq^{TM} Master Mix (Promega) as specified by the manufacturer.

Gene-specific primer pairs were used to generate products of 300-400 bp after 28 cycles. Products were analysed by electrophoresis on agarose gels as described (Huber and Zhao, 2010).

Gene specific primer pairs:

Nuclear actin (F): 5'CTCACCCTGAAGTATCCCATTG; (R): 5'GAAGCAGCTGTTGCCATTT

β−tubulin (F): 5'CCCAACAACGTTAAGACCG; (R): 5'CCTCCTCTTCCCCTTCCT

Cyclin B1 (F): 5"CTTTGGCTGGAAAGAGGGTTG; (R): 5'CTGACTGCTTGTGCATCCTCA

D7 (F): 5'CCCTAAACAGGAGCTTGATCTG; (R): 5'CTGCACCATGGGTTTGTATTTG

EF1α (F): 5'GGAGAATTTGAGGCTGGTATCT; (R) 5'GAGTCGTAGAGGCTTGTTAGTG

HDAC (F): 5"CGGTTACGGGATGGGATTGAC; (R): 5'GTTGGATGGGCTGATGTGGAAG

H1M (F): 5'CTGAGGGAGGCAACAAGGAAAAT; (R): 5'CTGCTCTGCATTTGGGTCTAC

Mos (F): 5'GTGGCGCTGAAGAAGGTAAA; (R): 5'ATAGGCCACTACCGCATAGA

Nanos1 (F): 5'CTGCAGCCTCAGAGAGAAGG; (R): 5'CCACACAAAGGGCAAGTGTA

rp-L14 (F): 5'GTCGTACCAACTCCAGTTTCA; (R): 5'GTAGACTTCACGGGCCTTAC

Vg1 (F): 5'CCATACCCGCTGACAGAAATA; (R): 5'CAGCTAACAGTCAAGGCAAATC

Xcat2 (F): 5'GCTTTGACTCATGGAGCGAC; (R): 5'GCCGAGTGAGACATCAGTGT

YB1 (F): 5'CAGTGTGGGAGATGGTGAAC; (R): 5'GAACTGGAGCATTGGAGTATTG

3. Results

3.1 Identification and expression of xRAPB

The original guinea pig antibody raised against recombinant RAP55 recognized three proteins in oocyte extracts from *Pleurodeles waltl* with apparent masses of 140, 68 and 56 kDa, but only one protein from *Xenopus laevis* with a mass of 52 kDa (Lieb et al., 1998). The 68 kDa protein was named RNA-associated protein 55 (the predicted mass of the sequenced clone being 55 kDa). The rabbit antibody raised against a 52 kDa protein isolated from *Xenopus* mRNP (Sommerville and Ladomery 1996) recognizes only the 52 kDa protein from *Xenopus* and the 56 kDa protein from *Pleurodeles* (Fig. 1A). Subsequent cDNA cloning, based on peptide analysis of the 52 kDa protein, eventually identified it as a shorter variant of RAP55, one which we named RapB/*x*RAPB (Weston and Sommerville, 2006; Marnef et al., 2009). The

relationships between these proteins, including a form identical to xRAPB but with a single internal deletion (xRAP42; Arthur et al., 2009), are indicated (Fig. 1B).

Immunoblotting of extracts from developing oocytes using anti-p52/anti-xRAPB shows highest reactivity with early stages (I-II), with decreasing signal as oogenesis proceeds (Fig. 1C, top panel). Quantitation of the encoding mRNA/oocyte mass by RT-PCR reveals a similar pattern (Fig. 1C, bottom panel). However, on a per oocyte basis, the amount of xRAPB-encoding mRNA increases through oogenesis, indicating that expression of xRAPB, itself, is subject to translational control.

Immunostaining of ovary sections with anti-xRAPB reflects the immunoblotting results, with reaction steadily decreasing from early stage to be low in concentration by late stage (Fig. 1D). It is also apparent that the cognate protein is almost exclusively cytoplasmic, as has been shown for RAP55/xRAPA (Tanaka et al., 2006).

Immunoblotting of oocyte fractions bound or unbound by oligo(dT)-cellulose shows that the protein detected by anti-xRAPB is bound to an extent similar to *bona fide* mRNP components, such as Xp54, YB2 and CPEB (Fig. 1E). Binding efficiency is similar in the presence of either Mg^{2+} or EDTA, conditions which may influence intermolecular associations. Xp54, YB2 and xRAPB continue to be present in the poly(A)$^+$ fractions after progesterone-induced maturation, but at lower levels. Immunoreaction with anti-ERK2 is shown as a non-mRNP control and with anti-pMAPK as an oocyte maturation marker.

All indications are that xRAPB is an integral component of mRNP particles, particularly of a major population present in early oocytes. That xRAPB is a stably-bound component of these particles can be shown by equilibrium gradient centrifugation of unfixed poly(A)$^+$ RNP through high salt (15-40% Cs_2SO_4). Immunoblotting of gradient fractions with a mixture of antibodies to recognize the major mRNP proteins shows that xRAPB together with Xp54 remain bound to RNA (at a buoyant density of 1.44 g.cm^3) after much of the YB2 has been stripped off and recovered at around 1.22 g.cm^3 (Fig.1F). That the density peak represents the core of mRNP particles is demonstrated by extraction of RNA from the gradient fractions and hybridization with labelled probes directed against a range of early-expressed mRNAs, panels of two of which, nucleolin and histone deacetylase (HDACm) are shown (Fig. 1F). Thus the vast majority of hybridization signal corresponds to the position of the xRAPB immunostaining signal. For comparison, particles containing all of the major mRNP proteins can be obtained within a single density peak at around

1.39 g.cm^3 on banding in CsCl gradients (Fig. 1F). This density in CsCl corresponds to a protein:RNA ratio approaching the value of 4:1 which is normally quoted for intact mRNP (Cummings and Sommerville, 1988). The differential removal of YB2, especially of YB2b, from mRNP in moderate salt conditions (1 M NaCl) has already been noted (Ladomery and Sommerville, 1996) and may help explain better retention of YB2 in CsCl than in Cs$_2$SO$_4$.

3.2 Comparison of interactions of xRAPA and xRAPB with Xp54

Previous results have indicated a direct interaction of *x*RAPB with Xp54 helicase, an interaction that is not evidenced in early-stage oocytes with *x*RAPA (Minshall et al. 2007). Here we extend these observations by examining protein-protein interactions that occur using *in vitro* synthesised *x*RAPA, *x*RAPB and Xp54 (Fig. 2A) and compare the results with those obtained through crosslinking of proteins within native RNP particles.

Interaction of *x*RAPB with Xp54 can be shown by reciprocal immunoprecipitation from combinations of the i*n vitro*-synthesized proteins. Incubation of *x*RAPB with Xp54 and *x*RAPA with Xp54 was followed by binding and elution from immobilized anti-Xp54 and anti-*x*RAPB. Autoradiographs show that anti-Xp54 co-precipitates *x*RAPB much more effectively than *x*RAPA (Fig. 2B, top) and that anti-*x*RAPB co-precipitates Xp54 with *x*RAPB but much less with *x*RAPA (Fig. 2B, bottom).

That *x*RAPB and p54 make close contacts *in vivo* can be shown by u.v.-crosslinking of native mRNP particles (Fig. 2C). Here, both *x*RAPB and Xp54 are found in complexes with identical mobilities on SDS-PAGE at about 110 kDa, even on using heat-treated pellets which lack YB2 and mRNA and are reacted simultaneously with anti-*x*RAPB and anti-Xp54. This M$_r$ value corresponds well with the interpretation of the formation of heterodimers. These complexes are not affected by ribonuclease treatment after irradiation. In comparison, other mRNP components (eg.YB2a/b) form differently-migrating complexes (right panel). Larger complexes running at the top of the gel and detected with anti-Xp54 and anti-YB2, but not with anti-*x*RAPB, are disaggregated on ribonuclease treatment. This observation suggests that *x*RAPB, unlike Xp54 and YB2, may have no direct RNA-binding activity.

These results indicate that, during early oogenesis, *x*RAPB is a natural partner protein for the RNA helicase Xp54, perhaps in selecting mRNAs for early translation.

3.3 xRAPB expression complements Xp54 expression in the formation of mRP particles

Once assembled and processed in the nucleus, YB2- and Xp54-bound transcripts become restricted to the cytoplasm (Smillie and Sommerville, 2002), possibly through anchoring by Scd6 proteins. In order to study the interaction of *x*RAPB and Xp54 in the presumed cytoplasmic addition of *x*RAPB to mRNP particles, recombinant forms of the proteins were expressed *in vivo* after injection into mid-stage, oocytes. T7-tagged Xp54 and myc-epitope-tagged *x*RAPB, or myc-epitope-tagged *x*RAPA, were co-expressed from CMV-driven vectors injected directly into oocyte nuclei. This approach has the advantage of accessing the complete, natural pathway of gene expression and therefore is more likely to produce correctly located and functioning proteins (Braddock et al., 1994; Matsumoto et al., 1998). The compositions of the three recombinant proteins, showing the location of their functional domains, are represented in Fig. 3A.

The relative rates of synthesis of the epitope-tagged proteins were compared with the levels of endogenous proteins by immunoblotting with anti-Xp54 and anti-*x*RAPB. It was found that equivalence for both was reached at between 24 h and 48 h post-injection of the relevant vector (Fig. 3B). Interestingly, for both proteins, as the level of tagged protein increased, the level of endogenous protein appeared to show a corresponding decline, indicating possible homeostatic regulation.

The shorter-term kinetics of co-expression of the recombinant proteins were examined by injecting run-off transcripts (using T3 or T7 polymerase) into the cytoplasms of mid-stage oocytes and sampling for immunoblotting at two-hourly intervals. As can be seen (Fig. 3C), myc-tagged-*x*RAPB is detected and accumulated from 4 h post-injection. However, co-expression with T7-tagged-Xp54 leads to earlier detection of both Xp54 and *x*RAPB (from 2 h). This co-operative effect was then exploited by examining mRNP assembly after nuclear co-injection.

As with co-precipitation of *x*RAPB and Xp54 from proteins synthesized *in vitro* (Fig. 2 B), immunoprecipitation from lysates of oocytes co-expressing myc-tagged *x*RAPB and T7-tagged Xp54 *in vivo*, showed co-precipitation using anti-myc epitope, anti-T7 epitope, anti-Xp54 or anti-*x*RAPB (Fig. 3D). Non-immune rabbit serum was used as a negative control. The extent of co-precipitation using anti-epitope tags to detect de novo-synthesized myc-*x*RAPB and T7-Xp54 corresponded well with co-precipitation results using antibodies directed against the native proteins. However,

antibodies recognizing Xp54 were more efficient in co-precipitating *x*RAPB than were the antibodies recognizing *x*RAPB in co-precipitating Xp54. This would be expected if Xp54 bound to *x*RAPB constitutes only a sub-fraction of the Xp54 population, assuming that the ectopically expressed proteins behave in a manner similar to their endogenous equivalents.

Stored mRNP particles typically sediment at 30-80S in rate-zonal gradients (Darnbrough and Ford, 1981). In order to check whether *x*RAPB is actively incorporated *in vivo* into newly-synthesized particles, epitope-tagged *x*RAPB and Xp54 were co-expressed in oocytes and their distribution was analysed after sedimentation in glycerol gradients. Assembly of newly synthesized *x*RAPB into mRNP particles was found to correspond (in size distribution) to that of newly synthesized Xp54 (Fig. 3E). Pre-treatment of the oocyte extract with ribonuclease resulted in both *x*RAPB and Xp54 being resolved in smaller molecular complexes. In contrast, *x*RAPA, co-expressed with Xp54, appeared to prevent Xp54 from entering into larger mRNP particles, again pointing to the co-operation of *x*RAPB and Xp54, but a dislocation of *x*RAPA and Xp54, in early mRNP assembly (Fig. 3F). It should be noted that immunostaining of all three components can be detected in pelleted post-80S material.

3.4 Comparison of the effects of knock-down and over-expression of xRAPA and xRAPB

Previous studies have shown that *Xenopus* *x*RAPA (RAP55) represses translation in an *in vitro* system and also *in vivo* in oocytes when tethered to a reporter RNA (Tanaka et al., 2006) as has Xp54 (Minshall et al. 2001, 2004). However, injection of anti-xRAPB IgG into oocytes does not interfere with the formation of masked mRNP particles, whereas injection of anti-Xp54 IgG releases masked reporter transcripts for translation (Braddock et al. 1994), indicating that *x*RAPB may not be a translation repressor. In order to explore this possibility, we compared the effects of knockdown and over-expression of *x*RAPB, *x*RAPA and Xp54. It has been generally assumed that stored mRNP particles are stable and accumulate until their protein products are required at the appropriate stage of development (reviewed, Weston and Sommerville, 2006). However, the formation and stability of maternal mRNP appears to involve a much more dynamic scenario. As expected, injection of anti-sense morpholinos (a/sMOs) into the cytoplasm of oocytes expressing recombinant *x*RAPB and Xp54

from nuclear vectors greatly inhibits their synthesis (Fig. 4A), but injection of a/sMOs directed against the endogenous mRNAs encoding these protein also results in significant inhibition (Fig. 4B). No significant MO cross-reactions were detected in comparing all of the targeted proteins. These findings open the possibility of using a/sMOs to examine the effects of depletion of *x*RAPB, *x*RAPA and Xp54 on translation rates in injected oocytes. As can be seen (Fig. 4C), Xp54 a/sMO significantly increases the rate of protein synthesis, whereas *x*RAPB a/sMO gives slight repression. The effect of *x*RAPA a/sMO differs little from the effect of a non-specific control MO. On comparing the spectrum of labelled proteins by SDS-PAGE / autoradiography (Fig. 4D, right panel) it can be seen that the a/sMO treatments result in differences of general signal intensity: there is no evidence for an increase or decrease in the translation of specific proteins. Also, comparison of the radiolabelling with protein staining in individual tracks indicates that the labelled bands do not fully correspond, either in intensity or migration. This reflects oocyte stage-specific translation and differential protein stability. Quantitation of track densities are shown in the accopanying table, again indicating that the most significant deviation from the control is the positive effect of anti-sense of Xp54 mRNA.

Results from the reverse experiment, examining the effect of increased expression of *x*RAPB, *x*RAPA and Xp54 on protein synthesis, are shown (Fig. 4E). Here there is a reversal of outcomes, with over-expression of Xp54 resulting in inhibition of protein synthesis and over-expression of *x*RAPB in an apparent activation. *x*RAPA gave no significant difference from the (mock-injected) control. The profiles of newly-synthesized proteins (Fig. 4F) again showed differences in overall intensity. In the autoradiograph shown, the last two track represents synthesis after co-expression of myc-*x*RAPB and T7-Xp54, which can be compared with the expression of these proteins individually. In these tracks the over-expressed myc-*x*RAPB can be discerned at its slower migrating position (white dot and upper arrow), whereas over-expressed T7-Xp54 is obscured in the heavier labelled region of the gel (white dot and lower arrow). Quantitation of track densities confirm a significant inhibition of translation by over-expressed Xp54 and a modest increase in translation of *x*RAPB (this is with the myc-*x*RAPB band contribution subtracted from the total). Co-expression with *x*RAPB with Xp54 leads to moderation of the repressor activity of Xp54 (Fig. 4F). The least we can conclude is that over-expresion of *x*RAPB does not inhibit the activity of already translating mRNAs.

3.5 xRAPB is associated with translating mRNAs

It might be expected that manipulated changes in translation rate would be reflected in changes in the distribution of mRNP particles, specifically in association with ribosomal components. Rate sedimentation analysis of extracts from mid-stage oocytes containing over-expressed Scd6 proteins show that the distribution of *x*RAPA remains typical of mRNPs containing endogenous Xp54 and YB2 (Fig. 5A, broken box area), whereas a significant proportion of the myc-*x*RAPB signal has moved into post-80S fractions not so well represented by Xp54 and YB2 (Fig. 5A, solid box area). The myc-*x*RAPB signal in faster sedimenting complexes is significantly weaker. The post-80S complexes are disassembled in the presence of EDTA (Fig. 5B).

Whereas mRNP particles from early- to mid-stage oocytes have been described as forming a heterogeneous size distribution on rate-sedimentation gradients (Darnbrough and Ford, 1981; Cummings and Sommerville, 1988), native *x*RAPB is seen to be present in particles with a bimodal distribution, sedimenting in sub-80S and post-120S fractions. This contrasts with Xp54 and YB2, both of which form a continuous distribution across the 80S region (Fig. 5C, broken box area) and indicates that mRNP particles free of *x*RAPB are present in mid-stage oocytes. On the other hand, the distribution of *x*RAPB seen here is typical of that of separated stored mRNP and polysomes. Hybridization of gene-specific antisense probes with RNA extracted from the gradient fractions confirms that mRNA not translated during early oogenesis (eg. encoding cyclin B1, Fig. 5C) is not present in putative polysome fractions but, instead, remains in fractions associated with stored mRNA. On the other hand, early-translated mRNA (eg. encoding β-tubulin, Fig. 5C) extends into the polysome region, reflecting the bimodal distribution of *x*RAPB. Support for these distributions representing a distinction between mRNP storage and translation complexes can be seen from gradients of the same extracts pre-treated with EDTA, which result in the total disruption of post-80S RNP with cyclinB1 mRNA now sedimenting with Xp54 and YB2 at less than 60S and the β-tubulin mRNA sedimenting at less than 40S with *x*RAPB (Fig.5D). The bimodal distribution of *x*RAPB is better defined in early-stage oocytes (Fig. 5E), whereas all post-80S signal is absent from ectopically-expressed *x*RAPB in late-stage and matured oocytes (Fig. 5F).

3.6 Identification of mRNA classes found in association with xRAPB

Confirmation of direct interaction of early-expressed mRNA species with *x*RAPB is obtained from RT-PCR of RNA extracted from immunoprecipitated RNP particles (Fig. 6). In order to standardize precipitation and to minimize potential immunological cross-reaction, both myc-tagged *x*RAPB and myc-tagged *x*RAPA were used as the targets for monoclonal anti-myc (cf. Huber and Zhao, 2010). As can be seen (Fig. 6), immunoprecipitates (P) from oocytes expressing myc-*x*RAPB contained mRNA species that are being translated in oocytes (for nuclear actin, β-tubulin, EF1a, ribosomal protein L14 and HDACm) but not stored mRNAs that are translated later at oocyte maturation (for cyclin B1 and c-mos), in the egg (for D7) and during early embryogenesis (for somatic YB1 and linker histone H1M). Actively translating mRNAs are not precipitated from oocytes expressing myc-*x*RAPA, whereas stored mRNAs are precipitated to varying extent. However, this analysis is complicated by instability of some stored mRNAs (eg. encoding cyclin B1 and c-mos), but not of translating mRNAs or embryo-expressed mRNAs (eg. for H1M), in myc-*x*RAPA-expressing oocytes. Additionally, mRNAs that pass through localization pathways in early- to mid-stage oocytes (encoding Xcat2 and Vg1) but are translationally repressed during oogenesis were also immunoprecipitated along with *x*RAPB.

(All results shown here were generated from the same cDNA templates, the original RNA extracts showing similar amounts of ribosomal RNAs, Fig. 6.) Furthermore, incorporation of ectopically-expressed *x*RAP proteins is to be expected to be more efficient in mRNP complexes with a greater rate of turnover.

4. Discussion

4.1 xRAP is an integral component of poly(A)$^+$RNP in early-stage oocytes

The protein composition of mRNP particles in early-stage oocytes was first defined by Darnbrough and Ford, 1981. Of the four most abundant proteins associated with poly(A)$^+$RNA, two were characterized later as cold-shock domain Y-box proteins (YB2: Deschamps et al., 1992; Murray et al.,1992), a third as the DEAD-box RNA helicase Xp54/Dhh1 (Ladomery et al., 1997) and the last as the Scd6 family protein described here as *x*RAPB. We we define the main features of *x*RAPB and how they

may contribute to differences in function from the other Scd6 protein also present in *Xenopus* oocytes, *x*RAPA. *x*RAPA is the homologue of RAP55 extesively studied in the cells of other vertebrates (Marnef et al., 2009).

Immunoblots with anti-Xp52/*x*RAPB show that the concentration of *x*RAPB decreases from early oogenesis to full-growth (Fig. 1C,E), a feature confirmed by immunostaining ovary sections (Fig. 1D), whereas the concentration of the translation repressor *x*RAPA increases during oogenesis (Tanaka et al., 2006). Cross-reacting antibodies clearly show this reciprocal expression pattern (Minshall et al., 2007). That *x*RAPB co-isolates with Xp54, YB2 and CPEB (Minshall et al., 2007) in association with polyadenylated mRNA (Fig. 1E) indicates that this mRNP may be capable of entering the translation pathway. These observations can be compared with the timing of transcriptional activity which starts at maximum in early oocytes and decreases towards full growth and of the steady-state level of mRNA that exists from mid to late oogenesis, maintaining the pool of stored mRNA required for translation during oocyte maturation and early embryogenesis (Sommerville, 1990). Thus the availability of *x*RAPB matches the timing of translation of poly(A)$^+$RNA to maximize oocyte growth, whereas the availability of *x*RAPA matches the accumulation of stored mRNA.

4.2 Interaction of xRAPB with the RNA helicase Xp54

The ability of Xp54 and *x*RAPB to interact with each other: as *in vitro*-synthesized proteins (Fig. 2B); as native proteins (Fig. 2C; Minshall et al., 2009): as over-expressed proteins (Fig. 3D), contrasts with a lack of comparable interaction of Xp54 with *x*RAPA. Furthermore, co-expression of Xp54 with *x*RAPB leads to stabilization of *x*RAPB synthesis (Fig. 3C) and incorporation of both proteins into mRNP particles with a heterogeneous range of sizes (Fig. 3E), whereas co-expression *x*RAPA with Xp54 leads to the incorporation of *x*RAPA to the exclusion of Xp54, at least in fast-sedimenting particles (Fig. 3F). All of these results confirm Xp54/*x*RAPB selectivity in the assembly of a specific class of mRNP particles during early- to mid-oogenesis.

During early oogenesis, YB2a/b are much more stable than Xp54 and *x*RAPB, which have similar turnover rates (Dixon and Ford, 1982). This reflects the inclusion of YB2a/b in mRNP particles that show continuing translation repression (longer term storage) and the inclusion of Xp54 and *x*RAPB in translation-ready mRNPs. Here we observed the reduction of YB2a/b in mRNP sedimentation classes that contain myc-

*x*RAPB (Fig. 5A) compared with the maintenance of YB2a/b in sedimentation classes in which native *x*RAPB is absent (Fig. 5C,E). Furthermore, the stability of the native Xp54/*x*RAPB/mRNA complex and removal of YB2a/b in high salt conditions (Fig. 1F) is consistant with this functional grouping. However, activation of protein synthesis in early-stage oocytes may require dislocation, or conformational change (Minshall et al., 2009), of Xp54 from target mRNAs (see Section 4.3). The modification/stimulus required to release Xp54 from mRNP for translation activation is not known, although Xp54 phosphorylation (Sommerville, 1990: Weston and Sommerville 2006) and *x*RAPB methylation (Matsumoto et al., 2012) can be considered.

4.3 Involvement of xRAPB in promoting translation

Evidence presented here, that over-expression of *x*RAPB can lead to an increase in the rate of amino acid incorporation (Fig. 4E,F), whereas knock-down suggests a decrease (Fig. 4C,D), contrasts with the predicted translation repression by Xp54 . However, ectopic expression of *x*RAPB tends to neutralize the repressor activity of ectopic Xp54 (Fig. 4F).

The observation of an increase in the sedimentation rate of myc-*x*RAPB-containing RNP particles to post-80S fractions (Fig. 4A) is consistent with release of the bound/masked mRNA to enter into a translation initiation complex. Such '90S' particles have been shown previously to contain, in addition to 80S ribosomes and poly(A)$^+$mRNP particles, charged tRNA$_{met}$ (Cummings and Sommerville, 1988). The transitions from repression to translation potentiation to translation may require sequential removal of masking and repressor proteins. Nevertheless, YB2 orthologues in mammalian cells (YB1/p50) and *Chironomus* cells (*ct*YB1) can remain associated with translating mRNAs, albeit with lower stoichiometry (Evdokimova and Ovchinikov, 1998; Soop et al., 2003). Thus, there is a precedent for core mRNP proteins being carried over into polysomes, as indicated with the detection of over-expressed *x*RAPB in post-80S (Fig. 5A) and of native *x*RAPB in the polysomal region of glycerol gradients (Fig. 5C,E). What is significant is that the translation repressor Xp54 does not accompany *x*RAPB in these translocations. Whether *x*RAPB plays a direct role in translational release is not clear. However, it is interesting to note that the Scd6 paralogue expressed in trypanosomes does not form a complex with the

p54/Dhh1 helicase (Cristodero et al., 2014), although this Scd6 protein, like *x*RAPA, acts as a translation repressor. In comparison, a fraction of *x*RAPB from early- to mid-stage oocytes, although apparently free of most of its accompanying Xp54 and YB2a/b, sediments in polysomal regions of glycerol gradients (Fig. 5A,E). The bimodal distribution formed is characteristic of free and translating mRNP, with all mRNP resolving to the free zone after treatment with EDTA (Fig. 5B). A similar situation has already been reported for ovarian tissue of *Drosophila*, where a proportion of the Scd6 protein Tral isolates with polysomes whereas the Dhh1 orthologue Me31B isolates only in free mRNP particles (Liu et al., 2011). In *Xenopus* oocytes, intermediate gradient *x*RAPB-free fractions contain both Xp54 and YB2, indicating an alternative class of mRNP. That this is the case is confirmed by the identification, by slot-blot hybridization, of RNA extracted from the gradient fractions (Fig. 5C). Whereas early-translated mRNA (eg. encoding β-tubulin) follows the distribution of *x*RAPB, stored mRNA (eg. encoding cyclin B1) is present in the intermediate zone. By late oogenesis and oocyte maturation, ectopically-expressed *x*RAPB is locates only in free (sub-80S) particles (Fig. 5F)

4.4 Identification of catagories of mRNA that bind xRAPB

That the translated mRNAs are indeed associated with *x*RAPB and not *x*RAPA is shown by analysis of RT-PCR products of RNA co-immunoprecipitated with *x*RAPB and *x*RAPA (Fig. 6). All of the sequences derived from translating mRNAs were detected in *x*RAPB co-precipitates and to a much lesser extent in *x*RAPA co-precipitates (Fig. 6, right column). Those tested included mRNAs encoding: structual proteins (oocyte-specific β-tubulin and nuclear actin); translation components (EF1α and ribosomal protein L14) and stored enzymes (maternal histone deacetylase, HDACm). In addition, however, a category of mRNAs that are not translated in oocytes was also immunoprecipitated along with *x*RAPB. These are mRNAs localized to the vegetal region in early-stage oocytes: encoding Xcat2/Nanos1 (Lai et al., 2011) and in mid-stage oocytes: encoding Vg1 (Kloc and Etkin, 2005). The co-precipitation of Vg1 mRNA with *x*RAPB is consistant with the previous demonstration that *x*RAPB, together with *x*RAPC (Fig. 1B), YB2 and Xp54 can be immunoprecipitated by antibodies recognizing Vg1-localizing proteins (Arthur et al., 2009). Here we have shown that early-localized particles containing Nanos1 mRNA appear also to contain

*x*RAPB. Since Nanos mRNA is specifically translated in the next generation of precursor germ cells, perhaps *x*RAPB, if still bound, is required for its early activation.

Of the mRNAs not co-precipitated with *x*RAPB (Fig. 6, left column), co-precipitation with *x*RAPA is also absent from those mRNAs not translated until egg formation (D7) or early embryogenesis (somatic YB1 and maternal linker histone H1M). Although the mRNAs to be translated during oocyte maturation (cyclinB1 and c-mos) do appear to have bound *x*RAPA, the mRNAs themselves appear to be unstable. This may well be due to the over-expression of *x*RAPA, known to be a component involved with Xp54 in the RNA degradation pathway. This highlights a potential limitation of the use of epitope-tagged proteins as a target for immunoprecipitation: although they present optimum antigenicity, their over-expression may lead to metabolic side-effects.

4. 5 mRNA storage versus translation and turnover

Induction of mRNA degradation by over-expressed RAP55/RAPA has been well documented for a wide range of organisms (Marnef et al., 2009) and in vertebrates appears to be essential for the formation of P-bodies. *Xenopus x*RAP55 (*x*RAPA) has been shown to be present in non-defined cytoplasmic foci in oocytes and to locate to P-bodies when expressed in mammalian cells (Tanaka et al., 2006). Furthermore, tethering of xRAP55 to a reporter mRNA expressed in late-stage oocytes caused a decrease in the levels of the reporter protein. However, early growth of mouse oocytes is accompanied by the loss of P-bodies and translocation of mRNP complexes (lacking decapping enzymes) to sub-cortical regions (Flemr et al., 2010). Also, the involvement of the Scd6 protein involved in mRNP storage granule formation in trypanosomes does not correlate with translation repression of granule-recruited mRNA (Kruger et al., 2013). Translationally silent mRNAs in the gametocytes of *Plasmodium* are contained in storage granules defined by the presence of the Dhh1 and Scd6 orthologues, DOZ1 and CITH, but the absence of RNA degradation factors (Mair et al., 2010). Thus germ cells, from single-celled organisms to those of multicelled organisms present a special case in the use of Dhh1 and Scd6 for mRNA storage and distribution rather than degradation.

The major feature of Scd6 proteins in oogenic/embryonic systems lies in their efficient handling of mRNA through the developmental programme. In *Xenopus*

oocytes, at least, this is managed through the involvement if different Scd6 proteins; *x*RAPA and *x*RAPB and possibly others. As argued here, *x*RAPB is responsible for the selective distribution and translation, from the total pool, of those mRNAs required for cell reorganization and growth, whereas *x*RAPA is required for translation repression and storage of those mRNAs required for late oogenesis and meiosis. Since RAPB paralogues are expressed in a wide range of organisms, including mouse and human, their further functions should be well worth investigating.

References

Albrecht, M. and Lengauer, T. (2004). Novel Sm-like proteins with long C-terminal tails and associated methyltransferases. FEBS Lett. **569**, 18-26.

Anantharaman, V. and Aravind, L. (2004). Novel conserved domains in proteins with predicted roles in eukaryotic cell-cycle regulation, decapping and RNA stability. BMC Genomics, **5**: 45.

Arthur, P. K., Claussen, M., Koch, S., Tarbashevich, K., Jahn, O., and Pieler, T. (2009). Participation of *Xenopus* Elr-type Proteins in Vegetal mRNA Localization during Oogenesis. J. Biol. Chem. **284**, 19982-19992.

Balagopal, V. and Parker, R. (2009). Polysomes, P bodies and stress granules: states and fates of eukaryotic mRNAs. Curr. Opin Cell Biol. **21**, 403-408.

Bouvet, P. and Wolffe, A. P. (1994). A role for transcription and FRGY2 in masking maternal mRNA within *Xenopus* oocytes. Cell **77**, 931-941.

Braddock, M., Muckenthaler, M., White, M.R.H., Thorburn, A.M., Sommerville, ,J., Kingsman, A.J. and Kingsman, S.M. (1994). Intron-less RNA injected into the nucleus of *Xenopus* oocytes accesses a regulated translation control pathway. Nucleic Acids Res., **22**, 5255-5264.

Cabada, M. O., Darnbrough, C, Ford P. J. and Turner, P. C. (1977). Differential accumulation of two size classes of poly(A) associated with messenger RNA during oogenesis in *Xenopus laevis*. Dev. Biol. **57**, 427-439.

Cristodero, M., Schimanski B., Heller, M. and Roditi, I. (2014). Functional characterization of the trypanosome translational repressor SCD6. Biochem J. **457**, 57-67.

Cummings, A. and Sommerville, J. (1988). Protein kinase activity associated with stored messenger ribonucleoprotein particles of *Xenopus* oocytes. J. Cell Biol. **107**, 45-56.

Darnbrough, C. H. and Ford, P. J. (1981). Identification in *Xenopus laevis* of a class of oocyte-specific proteins bound to messenger RNA. Eur. J. Biochem. **113**, 415-424.

Deschamps, S., Viel, A., Garrigos, M., Denis, H. and Le Maire, M. (1992). mRNP4, a major mRNA-binding protein from *Xenopus* oocytes is identical to transcription factor FRGY2. J. Biol. Chem. **267**, 13799-13802.

Dixon, L.K. and Ford, P.J. (1982). Regulation of protein synthesis and accunulation during oogenesis in *Xenopus laevis*. Dev. Biol. **93**, 478-497.

Evans, J.P. and Kay, B.K. (1991). Biochemical fractionation of oocytes. Methods Cell Biol. **36**, 133-148.

Evdokimova, V. M. and Ovchinikov, L. P. (1998). Translational regulation by Y-box transcription factor: involvement of the major mRNA-associated protein p50. Int. J. Biochem. Cell Biol. **31**,139-149.

Flemr, M., Ma, J., Schultz, R. M. and Svoboda, P. (2010). P-body loss is concomitant with formation of a messenger RNA storage domain in mouse oocytes. Biol. Reprod. **82**,1008-1017.

Huber, P.W. and Zhao, W. (2010). Detection of protein-RNA complexes in *Xenopus* oocytes. Methods **51**,82-86.

Kick, D., Barrett, P., Cummings, A. and Sommerville, J. (1987). Phosphorylation of a 60 kDa polypeptide from *Xenopus* oocytes blocks messenger RNA translation. Nucleic Acids Res. **15**, 4099-4109.

Kloc, M. and Etkin, L. D. (1995). Two distinct pathways for the localization of RNAs at the vegetal cortex in *Xenopus* oocytes, Development **121**, 287–297

Ko, S., Kawasaki, I. and Shim Y-H. (2013) PAB-1, a *Caenorhabditis elegans* Poly(A)-binding protein, regulates mRNA metabolism in germline by interacting with CGH-1 and CAR-1. PLoS ONE 8(12): e84798. doi:10.1371/journal.pone.0084798

Kozak, M. (2008). Faulty old ideas about translational regulation paved the way for current confusion about how microRNAs function. Gene **429**, 108-115.

Krüger, T., Hofweber, M. and Kramer, S. (2013). SCD6 induces ribonucleoprotein granule formation in trypanosomes in a translation-independent manner, regulated by its Lsm and RGG domains. Mol. Biol Cell. **2013**, 24, 2098-2111.

Ladomery, M., Wade, E. and Sommerville, J. (1997). Xp54, the *Xenopus* homologue of human RNA helicase p54, is an integral component of stored mRNP particles in oocytes. Nucleic Acids Res., **25**, 965-973.

Lieb, B, Carl, M., Hock, R., Gebauer, D. and Scheer,U. (1998). Identification of a novel mRNA-associated protein in oocytes of *Pleurodeles waltl* and *Xenopus laevis*. Exp. Cell Res., **245**, 272-281

Liu, L., Qi, H., Wang, J. and Lin, H. (2011). PAPI, a novel TUDOR-domain protein, complexes with AGO3, ME31B and TRAL in the nuage to silence transposition. Development **138**, 1863-1873

Mair, G.R. et al. (2010). Universal features of post-transcriptional gene regulation are critical for for Plasmodium zygote development. PLoS Pathog. **6**, 1-12 doi:10.1371.

Matsumoto, K., Meric, F. and Wolffe, A. (1996). Translational repression dependent on the interaction of the *Xenopus* Y-box protein FRGY2 with mRNA. J. Biol. Chem. **271**, 22706-22712.

Matsumoto, K., Wasserman, K. M. and Wolffe, A. P. (1998). Nuclear history of a pre-mRNA determines the translation activity of cytoplasmic mRNA. EMBO J. **17**, 2107-2121.

Matsumoto, K., Nakayama, H., Yoshimura, M., Masuda, A., Dohmae, N., Matsumoto, S. and Tsujimoto, M. (2012). PRMT1 is required for RAP55 to localize to processing bodies. RNA Biol. 2012 **9**, 610-623.

Marello K, J. LaRovere and Sommerville, J. (1992). Binding of *Xenopus* oocyte masking proteins to mRNA sequences. Nucleic Acids Res. **20**, 5593-5600.

Marnef, A., Sommerville, J. and Ladomery, M.R. (2009). RAP55: Insights into an evolutionarily conserved protein family. Interntl. J. Cell Biol. **5**, 977-981.

Marnef, A., Maldonado, M., Bugaut, A., Balasubramanian, S., Kress M., Weil D, Standart, N. (2010). Distinct functions of maternal and somatic Pat1 protein paralogs. RNA. **16**, 2094-2107.

Minshall, N. and Standart, N. (2004). The active form of Xp54 RNA helicase in translational repression is an RNA-mediated oligomer. Nucleic Acids Res., **32**, 1325-1334.

Minshall N., Thom, G. and Standart, N. (2001). A conserved role of a DEAD-box helicase in mRNA masking. RNA **7**, 1728-1742.

Minshall, N., Reiter, M.H. Weil, D. and Standart, N. (2007). CPEB interacts with an ovary-specific EIF4E and 4-ET in early *Xenopus* oocytes. J. Biol. Chem. **282**, 37389-37401.

Minshall, N., Kress, M., Weil, D. and Standart, N. (2009). Role of p54 RNA helicase activity and its C-terminal domain in translational repression, P-body localization and assembly. Mol. Biol. Cell **20**, 2464-2472.

Muller-McNicoll, M. and Neugebauer, K. M. (2013). How cells get the message: dynamic assembly and function of mRNA-protein complexes. Nature Rev. Gen. **14**, 275-287.

Murray, M.T., Schiller, D.T. and Franke, W.W. (1992) Sequence analysis of cytoplasmic mRNA-binding proteins of *Xenopus* oocytes identifies a family of RNA-binding proteins. Proc. Natl. Acad. Sci. USA **89**, 11-15.

Nakamura, Y., Tanaka, K.J., Miyauchi, M., Huang, L., Tsujimoto, M. and Matsumoto, K. (2010). Translational repression by the oocyte-specific protein P100 in *Xenopus*. Dev. Biol. **344**, 272-283.

Ryan, J. P., Llinas,A. J., White, D. A., Turner, B. M. and Sommerville, J. (1999). Maternal histone deacetylase is accumulated in the nuclei of *Xenopus* oocytes as protein complexes with potential enzyme activity. J. Cell Sci. **112**, 2441-2452.

Sheets, M.D., Fritz, B., Hartley, R.S. and Zhang, Y. (2010). Polyribosome analsis for investigating mRNA translation in *Xenopus* oocytes. Methods **51**, 152-156.

Smillie, D.A. and Sommerville, J. (2002). RNA helicase p54 (DDX6) is a shuttling protein involved in nuclear assembly of stored mRNP particles. J. Cell Sci., **115**, 395-407.

Sommerville, J. (1990.) RNA-binding phosphoproteins and the regulation of maternal mRNA in *Xenopus*. J. Reprod. Fert. Suppl. **42**, 225-233.

Sommerville,J. (1999). Activities of cold-shock domain proteins in translation control. Bioessays, **21**, 281-297.

Sommerville, J. (2010). Using oocyte nuclei for studies on chromatin structure and gene expression. Methods **51**, 157-164.

Sommerville, J. and Ladomery, M. (1996). Transcription and masking of mRNA in germ cells: involvement of Y-box proteins. Chromosoma **104**, 469-478.

Soop, T., Nashchekin, D., Zhao, J, Sun, X., Alzhanova-Ericsson, A. T., Björkroth, B., Ovchinnikov, L. and Daneholt, B. (2003). A p50-like Y-box protein with a putative translational role becomes associated with pre-mRNA concomitant with transcription. J Cell Sci. **116**, 1493-503.

Tanaka, K.J., Ogawa, K., Takagi, M., Imamoto, N., Matsumoto, K. and Tsujimoto, M. (2006). RAP55, a cytoplasmic mRNP component, represses translation in *Xenopus* oocytes. J. Biol. Chem. **281**, 40096-40106.

Weston, A. and Sommerville, J. (2006). Xp54 and related (DDX6-like) RNA helicases: roles in messenger RNP assembly, translation regulation and RNA degradation. Nucleic Acids Res. **34**, 3082-3094.

Yurkova, M. S. and Murray, M. T. (1997). A translation regulatory particle containing the *Xenopus* oocyte Y-box protein mRNP3+4. J. Biol. Chem., **272**, 10870-10876.

Figure legends

Fig. 1. Identification and expression of *x*RAPB **(A)** Immunoblot of poly(A)$^+$ fractions from oocytes of *Xenopus laevis* and *Pleurodeles waltl* reacted with guinea pig anti-RAP55 and rabbit anti-RNP2/Xp52. **(B)** Alternative designations of the two *Xenopus* Scd6 proteins described here (right panel) and percentage identities of the three proteins described to date. **(C)** Comparison of expression through oocyte stages of Xp52 and the RT-PCR products of the mRNA encoding Xp52. **(D)** Immunostaining of ovary section with anti-RNP2 showing reaction with stages I – IV. Perimeters of the stage III and IV oocytes are indicated by white outlines. Bar indicates 200 μm. **(E)** Immunoblot of extracts from previtellogenic (stage I) oocytes and mature oocytes, unbound (UB) and bound (B) by oligo(dT) cellulose. Lysates were obtained in the presence of 2mM Mg$_2$Cl or 5 mM EDTA. The transfer was reacted serially with anti-RNP2 (recognizing *x*RAPB); anti-Xp54; anti-RNP1 (YB2) ; anti-CPEB; anti-ERK2 and anti-phosphorylated MAPkinase (pMAPK). **(F)** Immunoblot of density gradient fractions of poly(A)$^+$ RNP reacted with anti-RNP1 (YB2) and anti-RNP2 (*x*RAPB). Slot blots of RNA extracted from the same fractions (lower panels) were reacted with ^{32}P-labelled anti-sense probes recognizing the mRNAs of nucleolin and histone deacetylase (HDAC).

Fig. 2. Interactions of *x*RAPB and *x*RAPA with Xp54. **(A)** Autoradiographs of SDS-PAGE gels showing *in vitro* interactions of ^{35}S-labelled recombinant proteins. The proteins were synthesized and labelled by coupled transcription/translation using cloned cDNAs in a reticulocyte lysate system (left panel). Single and mixed products were incubated and subjected to u.v.-cross-linking (UV) and/or digestion with ribonuclease A (RNase; 1 mg/ml). Large complexes are trapped at the top of the gels (arrows). Interactions resulting from mixtures of *x*RAPA and Xp54 (middle panel) and *x*RAPB and Xp54 (right panel) are shown. Percentage depletion of each component from its monomer band due to uv.-treatment, or partial recovery due to ribonuclease treatment, are shown beneath each track. **(B)** Immunoprecipitations of ^{35}S-labelled *x*RAPB/Xp54 and *x*RAPA/Xp54 mixes with immobilized anti-Xp54 and anti-RNP2. Bound (B) and unbound (UB) fractions. **(C)** Immunostained transfers from SDS-PAGE gels of oocyte poly(A)$^+$ RNP, untreated and u.v.-cross-linked (UV) with subsequent digestion with ribonuclease A. Putative, cross-linked Xp54/*x*RAPB heterodimers (~110 kDa) are recognized by anti-Xp54 and anti-RNP2. The two other

major mRNP proteins, FRGY2a/b, are not detected in cross-linked complexes with this same mobility.

Fig. 3. Complementation of *x*RAPB and Xp54 in the formation of mRNP particles. **(A)** Recombinant proteins produced from expression vectors used in this study. **(B)** Time course of translation *in vivo* from RNA transcripts encoding myc-tagged *x*RAPB, with and without co-translation of Xp54. The RNA was injected into the cytoplasm of stage III oocytes. **(C)** Immunoprecipitation from lysates of oocytes co-expressing *x*RAPB and Xp54. Expression vectors encoding epitope-tagged proteins (Fig. 3A) were injected into the nuclei of stage IV oocytes, which were incubated for 36 h before extraction. Proteins were unbound (UB) or bound (B) to immobilized anti-myc, anti-T7, anti-RNP2 or anti-Xp54 and separated by SDS-PAGE. The transfer was serially reacted with anti-RNP2 and anti-Xp54. **(D and E)** Sedimentation analysis of mRNP particles formed during the co-expression of *x*RAPB and Xp54 and *x*RAPA and Xp54. Glycerol gradient fractions were separated by SDS-PAGE and immunoblotted using first anti-myc, then anti-T7. Equal volumes of extracts were pre-treated with ribonuclease A (+RNase) prior to sedimentation. Ribosomal monomers sediment to the bottom of the centrifuge tubes, the pellet also containing larger complexes (80S+).

Fig. 4. Effects of knock-down and over-expression of *x*RAPA and *x*RAPB on translation rate and mRNP size distribution. **(A)** Effect of antisense morpholinos (a/sMOs) recognizing the translation start sites of endogenous *x*RAPB and Xp54 at 24 and 48h after cytoplasmic injection into stage III oocytes. Control is a random sequence MO. **(B)** Effect of a/s MOs on co-expressed myc-*x*RAPB and T7-Xp54. Vector injections as for Fig. 4B with MO injections after 12 h. **(C)** Effect of a/sMOs recognizing *x*RAPA (A), *x*RAPB (B), Xp54 (P) on the rate of amino acid incorporation. Oocytes were injected with MOs were incubated for 12 h before addition of [^{35}S]-methionine to the medium. Oocytes from each set were recovered at hourly intervals and processed to obtain percentage of radioactivity incorporated into protein. Data from three separate experiments were used to obtain means and standard dev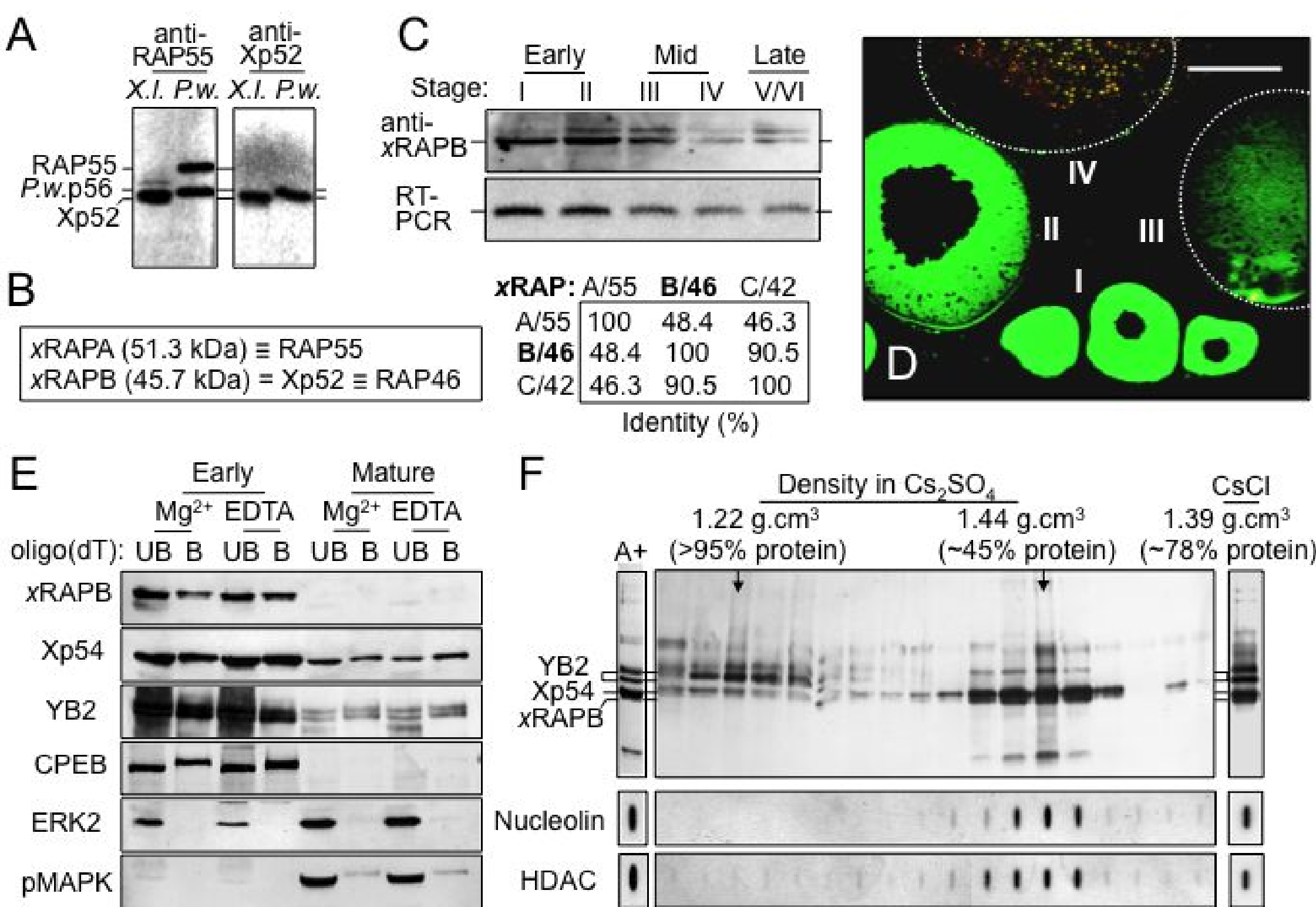iations. Autoradiographs of SDS-PAGE separated proteins were also obtained (panel on right). **(D)** As for **(C)** but 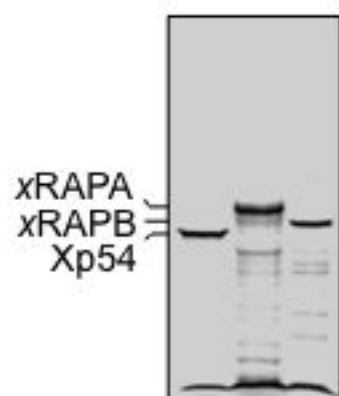with nuclear injection of expression vectors replacing MO injection. Bands attributed to the ectopically-expressed proteins were

subtracted from measurement of intensity totals (white spots). **(E)** Sedimentation analysis of extracts from stage IV oocytes, expressing either myc-*x*RAPA (upper panels) or myc-*x*RAPB (lower panels). Gradient fractions separated by SDS-PAGE and immunoblotted with anti-myc, anti-Xp54 and anti-RNP1 (YB2). Fastest sedimenting mRNP fractions containing myc-*x*RAPA are boxed in blue, and those containing myc-*x*RAPB are boxed in red. **(F)** As **(E)** but with 5mM EDTA replacing 2mM Mg^{2+}. Peak sedimentation of ribosomal monosomes (80S) and sub-units (60S and 40S) are indicated as rate markers.

Fig. 5. Properties of native *x*RAPB relating to early translation. **(A)** Sedimentation analysis of extract from stage III oocytes treated with 50 μg/ml cycloheximide (CHX). Gradient fractions were separated by SDS-PAGE and immunoblotted with anti-RNP2 (*x*RAPB), anti-Xp54 and anti-RNP1 (YB2). Fractions of mRNP lacking *x*RAPB are boxed in red. RNA extracted from aliquots of each of the gradient fractions was applied to a membrane by slot-blotting, the blot being subsequently hybridized with radio-labelled probes, antisense to mRNA encoding oocyte-specific β-tubulin and cyclin B1. Autoradiographs are shown (bottom panels). **(B)** As **(A)** but with 5mM EDTA replacing cycloheximide. **(C)** Hybridizations were also performed using transfers after RNA gel electrophoresis, the samples being obtained from total RNA (T), its polysomal pellet (P) and its non-polysomal supernatant (S). Probes used in autoradiographs shown are anti-sense to mRNA encoding ribosomal protein S27 (top panel) and FRGY1 (bottom panel). **(D)** Analysis of mRNAs immunoprecipitated (IP) by anti-myc from extracts from oocytes expressing *x*RAPA or *x*RAPB. RNA extracted from unbound (UB) and bound (B) fractions was used as templates for RT-PCR, amplification using gene-specific primers for *X. laevis* oocyte β-tubulin, histone deacetylase HDACm, cyclin B1 and maternal linker histone H1M. Products are separated on 1.5% agarose gels. Ribosomal RNAs (28S+18S and 5S) isolated from the same IP fractions are also shown (bottom panels).

A

anti-RAP55 | anti-Xp52
X.l. P.w. | X.l. P.w.

RAP55
P.w.p56
Xp52

B

xRAPA (51.3 kDa) ≡ RAP55
xRAPB (45.7 kDa) = Xp52 ≡ RAP46

C

Stage: Early (I, II) Mid (III, IV) Late (V/VI)

anti-xRAPB

RT-PCR

xRAP:	A/55	**B/46**	C/42
A/55	100	48.4	46.3
B/46	48.4	100	90.5
C/42	46.3	90.5	100

Identity (%)

D

I, II, III, IV

E

Early | Mature
Mg^{2+} | EDTA | Mg^{2+} | EDTA
oligo(dT): UB B | UB B | UB B | UB B

xRAPB
Xp54
YB2
CPEB
ERK2
pMAPK

F

Density in Cs$_2$SO$_4$
1.22 g.cm^3 (>95% protein) 1.44 g.cm^3 (~45% protein) CsCl 1.39 g.cm^3 (~78% protein)

A+

YB2
Xp54
xRAPB

Nucleolin

HDAC

A

B
IP: anti-Xp54
Mix: xRAPB+Xp54   xRAPA+Xp54
Fraction: UB   B   UB   B
xRAPA
xRAPB
Xp54

IP: anti-xRAPB
Mix: xRAPB+Xp54   xRAPA+Xp54
Fraction: UB   B   UB   B
xRAPA
xRAPB
Xp54

C
ā-Xp54   ā-xRAPB   ā-Xp54+   ā-YB2
                    ā-xRAPB
UV: − + +   − + +   − + +   − + +
RNase: − − +   − − +   − − +   − − +

~110
kDa

mono-
mers

p(A)⁺RNP   p(A)⁺RNP   HTP   p(A)⁺RNP

A

T7-Xp54 N [T7-tag] [NLS] [NES] Helicase [P] C 55.1 kDa

myc-*x*RAPA N [6Myc-tag] [Sm1/2] RGG FDF RGG RGG C 61.4 kDa

myc-*x*RAPB N [6Myc-tag] [Sm1/2] R-rich C 55.8 kDa

B

anti-Xp54   12   24   48 h
T7-Xp54
endo-Xp54

anti-*x*RAPB   12   24   48 h
myc-*x*RAPB
endo-*x*RAPB

C

Over-expression: myc-*x*RAPB   myc-*x*RAPB + T7-Xp54

0 2 3 4 6   0 2 3 4 6 h

anti-myc

anti-T7

D

myc-*x*RAPB + T7-p54

ā-myc   ā-T7   ā-*x*RAPB   ā-Xp54   NI

UB B   UB B   UB B   UB B   UB B

anti-myc

anti-T7

E

myc-*x*RAPB + T7-Xp54   80S+

anti-myc

+RNase

anti-T7

+RNase

F

myc-*x*RAPA + T7-Xp54   80S+

anti-myc

+RNase

anti-T7

+RNase

A myc-*x*RAPB + T7-Xp54

a/s MOs: control pCS-myc pCGT-T7
Time: 12 24 48 24 48 24 48 h

myc-*x*RapB

T7-p54

B endogenous

a/s MOs: control *x*RAPB Xp54
Time: 12 24 48 24 48 24 48 h

*x*RapB

Xp54

C a/s MOs

^{35}S-Met incorporation

P
A
C
B

Time (h)

D

Track density	
a/s MO	% Control
Control:	100
*x*RAPA:	97.6 ± 8.3
Xp54:	128.9 ± 17.8
*x*RAPB:	84.5 ± 14.3

St C A P B

E over-expression

^{35}S-Met incorporation

B
C
A
P

Time (h)

F

Track density	
Vector	% Control
Control:	100
Xp54:	43.6 ± 13.5
*x*RAPB:	109.7 ± 2.1
*x*RAPB + Xp54:	65.2 ± 7.0

St C P B B+P

A
+ Mg²⁺
80 S
myc-xRAPA
Xp54
YB2
myc-xRAPB
Xp54
YB2

B
+ EDTA
40 S
60 S
80 S

C
+ Mg²⁺
80 S
xRAPB
Xp54
YB2
β-tubulin
cyclinB1

D
+ EDTA
80 S

E
+ Mg²
80 S
xRAPB
Xp54
YB2

F
+ Mg²
80 S
myc-xRAPB
Xp54
YB2

IP anti-myc-
*x*RAPA *x*RAPB
UB B UB B

β-tubulin
N-actin
EF1α   Oocyte growth
rp-L14
HDACm

Xcat2/Nanos1   Oocyte mRNA localization
Vg1

IP anti-myc-
*x*RAPA *x*RAPB
UB B UB B

cyclin B1   Oocyte maturation
Mos

D7   Egg

YB1   Embryo-genesis
H1M

28+18S   rbRNA in samples
5S